

Controlled synthesis of monodispersed superparamagnetic nickel ferrite nanoparticles

P. Deb^{a,*}, A. Basumallick^b, S. Das^a

^a Department of Physics, Tezpur University, Tezpur 784028, India

^b Department of Metallurgy and Materials Engineering, Bengal Engineering and Science University, Shibpur, Howrah 711103, India

Received 22 December 2006; received in revised form 8 March 2007; accepted 21 April 2007 by D.D. Sarma

Available online 29 April 2007

Abstract

Nickel ferrite nanoparticles have been prepared through a gentle chemistry route, starting from iron nitrate, nickel nitrate and stearic acid. The nickel ferrite crystalline phase, the particle size and shape, and the homogeneity of the resulting nanoparticles were studied by X-ray diffraction and transmission electron microscopy. Fourier transform infrared techniques were used to study the composition characteristics of the as-prepared sample. Magnetization studies at room temperature showed superparamagnetic behavior for the nanoparticles. Magneto-optic rotation studies at different wavelengths of He–Ne lasers reveal non-linear behavior.

© 2007 Elsevier Ltd. All rights reserved.

PACS: 75.50.Tt; 75.75.ta; 81.40.Gh; 75.60.-d; 78.20.Ls

Keywords: A. Nanoparticles; B. Controlled synthesis; D. Superparamagnetic; E. Non-linear magneto-optic rotation

1. Introduction

The increasing demand for oxide nanoparticles for use as hard magnetic materials in ultra high density magnetic storage media has laid emphasis on their preparation and characterization because of their interesting and unusual physical properties [1–5]. Among these oxide nanoparticles, magnetic ones are the subjects of numerous interests due to their wide range of potential applications, from recording media to biological tagging [6–10]. Ferrites, the most widely used magnetic oxides, exhibit interesting magnetic, electrical and optical properties. Despite their physical resemblance to ceramics, ferrites are unique among magnetic materials because of their outstanding magnetic properties at high frequency, along with their very high resistivity and inherent high corrosion resistance. Though intense research effort has been carried out on zinc, cobalt and barium ferrites/doped ferrites, the study of nickel ferrite nanoparticles is yet to be exploited [11–13]. It is commonly known that nanoparticles

with controlled size and composition are of fundamental and technological interest. The preparation method determines not only the products characteristics like size and shape, but also their physical properties. Therefore, we report here the synthesis of nickel ferrite nanoparticles through a novel, simple, cost-effective and gentle chemistry route. The ability to obtain single-phase nickel ferrite magnetic nanoparticles with controllable particle size and size distribution will enhance its acceptability in wide range of magnetic and magneto-optical devices.

2. Experimental

Initially, a homogeneous solution was prepared by melting stearic acid at 80 °C and adding ferric nitrate $\text{Fe}(\text{NO}_3)_3 \cdot 9\text{H}_2\text{O}$ and nickel nitrate $\text{Ni}(\text{NO}_3)_2 \cdot 6\text{H}_2\text{O}$ in suitable proportion. All the reagents used for the experiment were of analytical reagent grade. A reddish brown solution was formed which was stirred continuously at 125 °C for two hours until all the brown fumes of NO_2 evolved out of the solution. A reddish brown viscous mass was formed, which was allowed to cool in air. The solidified mass so obtained was treated with 80 ml tetrahydrofuran (THF) and stirred intensely for 15 min followed

* Corresponding author. Tel.: +91 03712 267007x5560; fax: +91 03712 267006.

E-mail address: pdeb@tezu.ernet.in (P. Deb).

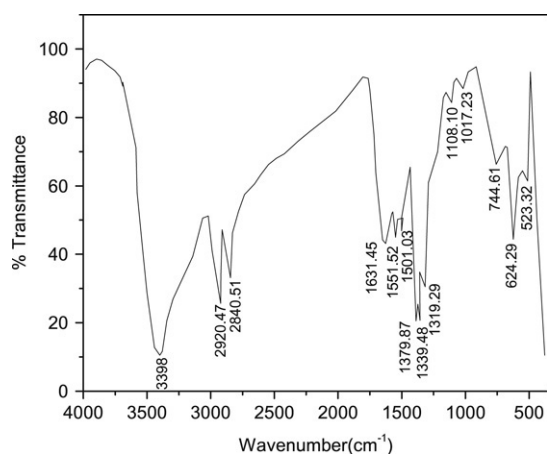


Fig. 1. FTIR spectrum of the as-prepared powder precipitates.

by centrifugation. The precipitated mass was then dried at 70 °C in air oven for 10 h. Nanosized nickel ferrite particles were obtained by heating the as-prepared sample inside an electrically heated furnace at the temperature 300 °C. The desired temperature of the furnace was controlled by a PID controller with an accuracy up to ± 1 °C. Fourier transform infrared spectroscopy (FTIR) studies were carried out on the as-prepared sample to examine the compositional characteristics. Microstructural characterization of the heat-treated sample was studied by X-ray diffraction (XRD) using $\text{CoK}\alpha$ radiation from a Philips PW-1830 diffractometer at 35 kV and 25 mA. Despite the fact that transmission electron microscopy (TEM) studies yield only a overall estimate about the particle size distribution, this technique was used to supplement the results of XRD studies. The magnetic characteristics, e.g. $M-H$ and $M-T$ plots of the samples, were also studied. The magneto-optic characterization of the so-prepared samples in polyvinyl alcohol (PVA) medium was studied for three different wavelengths of He–Ne laser beams.

3. Results and discussion

The chemical and compositional characteristics of the as-prepared powder precipitates were analyzed by FTIR spectroscopy. Fig. 1 represents the FTIR spectrum of the

as-prepared powder particles in KBr. The bands with the peaks at 535.93, 675.07 and 814.21 cm^{-1} are assigned to the deformation vibration of Fe–OH groups and the peak observed at 3398.66 cm^{-1} is assigned to the stretching vibration of these groups [14]. The bands with peaks observed at 1044.51 and 1114.88 cm^{-1} can be assigned to O–H bending vibration [15]. The 1313.19, 1343.58 and 1383.56 cm^{-1} peaks are attributed to the characteristic $-\text{CH}_3$ bending. The band observed between 1480 and 1700 cm^{-1} indicate the presence of nitro compounds [15,16]. The peaks at 2840.51 and 2920.47 cm^{-1} are due to C–H stretching vibration [15,16]. The above spectroscopic observation suggests that the as-prepared sample consists of an intermediate/complex of stearates, nitro compounds and residual stearic acid.

XRD studies were carried out on an as-prepared sample and on a powder sample heat treated isothermally at 300 °C for 1 h. The XRD pattern of the as-prepared sample shown in Fig. 2(c) does not exhibit any significant crystalline peak, which corroborates the inferences drawn from the FTIR spectroscopic studies. The XRD pattern of the heat-treated sample (see Fig. 2(b)) shows the presence of nickel ferrite only [17]. Hence, heat-treating the as-prepared sample in air causes complete decomposition of the organic compounds and evolution of nickel ferrite particles. A pattern decomposition procedure using a pseudo-Voigt profile shape function [18] and subsequent single line analysis based on the equivalent Voigt representation [19] was used for the determination of crystalline size and microstrain in the crystallite. The volume-weighted mean crystalline size of nickel ferrite has been found to be 9 nm for the sample heat treated at 300 °C for 1 h, and the corresponding lattice strain is 0.65. The XRD pattern of the sample heat treated at 400 °C exhibits the presence of NiO [20] and $\alpha\text{-Fe}_2\text{O}_3$ [21] along with NiFe_2O_4 peaks (refer Fig. 2(a)). Hence with 400 °C heat treatment, NiFe_2O_4 decomposes to NiO and $\alpha\text{-Fe}_2\text{O}_3$. Hence further characterization studies have been carried out on the sample heat treated at 300 °C which consists of NiFe_2O_4 only.

Fig. 3(a) shows a TEM photograph of the sample obtained after heating the sample at 300 °C. The particle size distribution and subsequently the average particle size were evaluated from the TEM micrograph by counting around 100 particles. The estimated particle size distribution (see Fig. 3(b)) for the sample

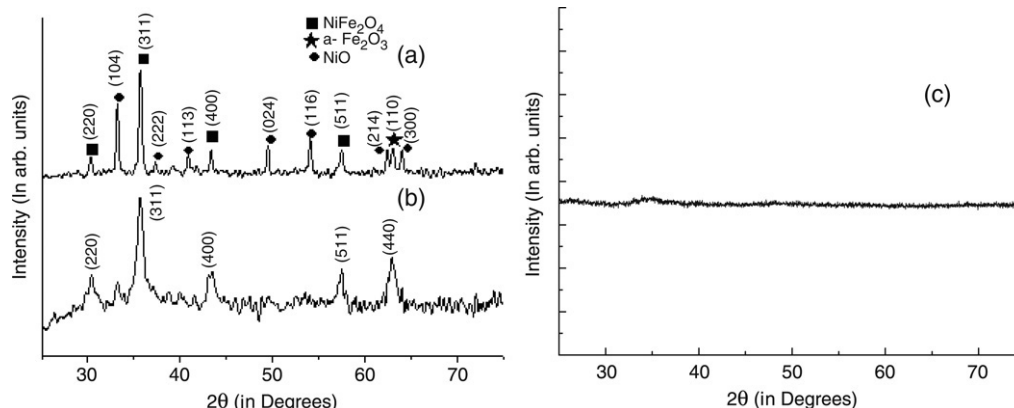


Fig. 2. XRD pattern of the (a) powder sample heat treated at 400 °C, (b) powder sample heat treated at 300 °C and (c) as-prepared powder.

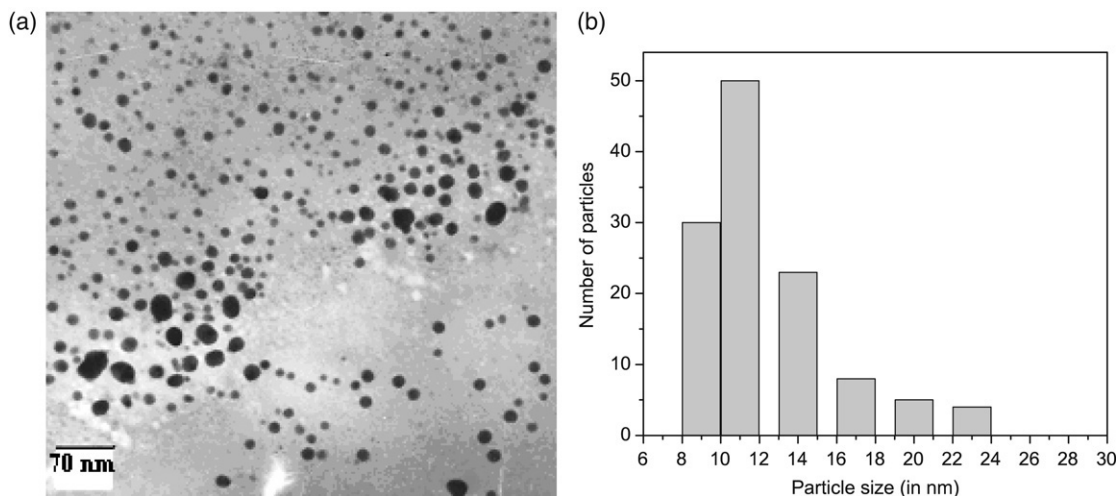


Fig. 3. (a) TEM photograph of the sample obtained after heat treatment at 300 °C and (b) the estimated particle size distribution.

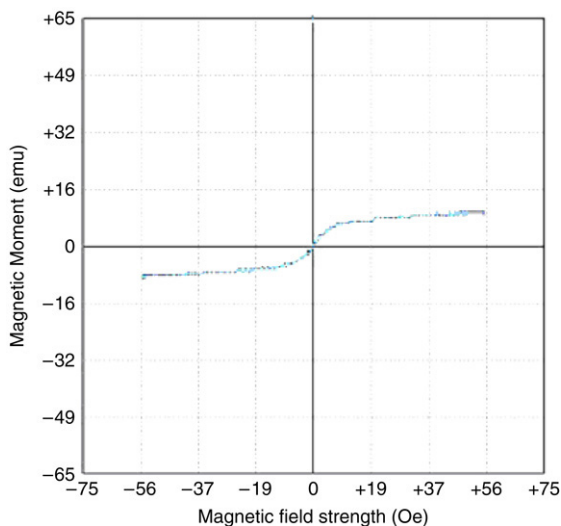


Fig. 4. Hysteresis loop for the sample heat treated at 300 °C.

has been found to be narrow, and it lies within the range ~ 8 – 24 nm. The average particle size measured has been found to be ~ 11 nm, which is in close agreement with the XRD results.

Fig. 4 shows the hysteresis loop plot for the sample heat treated at 300 °C for 1 h. Interestingly, it has been revealed from the loop that the coercivity and remanence are almost zero and the saturation magnetization value is 9.74 emu/g. This is a characteristic of superparamagnetism [22]. The Curie temperature, as obtained from the M – T plot, is around 210 °C. These values are significantly different from the values for bulk nickel ferrite particles reported elsewhere [23].

The magneto-optic rotation in varying magnetic field for nickel ferrite nanoparticles embedded in polyvinyl alcohol (PVA) was studied for three different color He–Ne lasers (refer Fig. 5). For such a study, an optical medium is prepared by dispersing nickel ferrite nanoparticles in PVA solution. First, 20 ml of distilled water is taken and heated to 70 °C until a PVA and water solution is formed. Then, 0.25 g of the sample heat treated at 300 °C is added to the PVA solution and

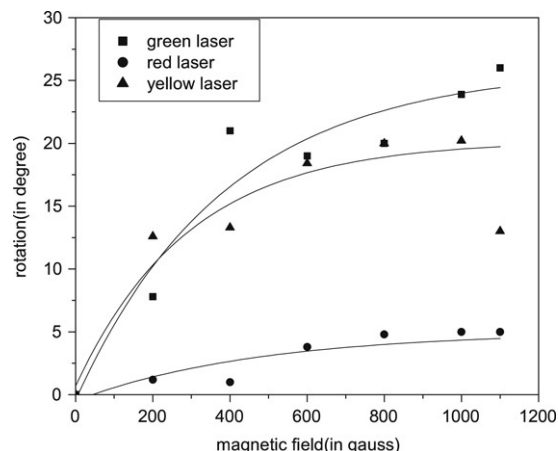


Fig. 5. Magneto-optic rotation versus magnetic field for heat-treated nanoparticles in PVA medium.

stirred continuously until a brown viscous gel is formed. Then, the magneto-optic rotation characteristic is studied. Initially, the rotation increases linearly with the increase in magnetic field and later it becomes almost constant. The non-linear behavior of superparamagnetic nickel ferrite clusters can be explained by assuming the presence of an anisotropic axis along which ferrite nanoparticles align. Here, superparamagnetic nickel ferrite particles have an asymmetric distribution in the matrix of PVA. Since these ferrites nanoparticles are randomly dispersed inside the PVA matrix, but with a preferred orientation along “anisotropy” axis, the external magnetic field is exerting a torque. A preferred orientation should arise during cluster formation as a consequence of magnetic or electrostatic interaction between the ferrite nanoparticles and the applied magnetic field or because of interaction between the ferrite particles and the PVA matrix. Considering the equilibrium between the electrostatic interaction and the magnetic torque, a phase lag “ φ ” should exist between the magnetic field and the anisotropy axis, which for small angles is proportional to the applied torque. Since the torque tends to orient the magnetic dipole parallel to the “anisotropy” axis and to the external magnetic field, the amplitude of the rotation of magnetic dipoles

linearly depends on the magnetic field for small magnetic fields. At higher magnetic fields, the clusters are acting as units themselves rather than the particles composing the clusters. Hence, when rotated, the clusters behave as a permanent magnetic dipole. Therefore, the rotation with the increase in magnetic field tends to attain the saturation value. Moreover, the magneto-optic values for a particular applied magnetic field change with the change in laser light. The Verdet constant for the nickel ferrite nanoparticles in PVA medium for different He–Ne laser light has been calculated by using the slope of the linear portion of the curves, and the values obtained are 1.616, 0.22 and 0.21 respectively for red, yellow and green laser lights.

4. Conclusion

The reported synthesis method is suitable for the preparation of monodispersed nickel ferrite nanoparticles. The compositional characteristics reveal the presence of an intermediate/complex of stearates, which decomposes and liberates nickel ferrite on heat treatment. XRD line profile analysis and TEM studies confirm the presence of nickel ferrite nanoparticles with average particle size ~ 10 nm and corresponding microstrain 0.65%. Superparamagnetic behaviour is obtained in the samples. Non-linear behavior of magneto-optic rotation characteristics is observed with varying magnetic field for the nanoparticles in PVA medium.

References

- [1] A.K. Gupta, M. Gupta, *J. Biomaterials*. 26 (2005) 3995.
- [2] M. Sugimoto, *J. Amer. Ceram. Soc.* 82 (2) (1999) 269.
- [3] Y. Xia, P. Yang, Y. Sun, Y. Wu, B. Mayers, B. Gates, Y. Yin, F. Kim, H. Yan, *Adv. Mater.* 5 (2003) 15.
- [4] Z.L. Wang, *Adv. Mater* 5 (2004) 15.
- [5] C.N.R. Rao, G.U. Kulkarni, P.J. Thomas, V.V. Agrawal, U.K. Gautam, M. Ghosh, *Current Sci.* 85 (2003) 7.
- [6] Q.A. Pankhurst, J. Connolly, S.K. Jones, J. Dobson, *J. Phys. D: Appl. Phys.* 36 (2003) R167.
- [7] P. Tartaj, M.P. Morales, S.V. Verdaguier, T.G. Carreno, C.J. Serna, *J. Phys. D: Appl. Phys.* 36 (2003) R182.
- [8] C.C. Berry, A.S.G. Curtis, *J. Phys. D: Appl. Phys.* 36 (2003) R198.
- [9] S. Mornet, S. Vasseur, F. Grasset, E. Dugnet, *J. Mater. Chem.* 14 (2004) 2161.
- [10] R. Mendoza-Resendez, M.P. Morales, C.J. Serena, *Mater. Sci. Eng. C* 23 (2003) 1139.
- [11] P. Deb, S. Ghosh, A. Basumallick, N.R. Bandyopadhyay, *Indian J. Phys.* 78(A) (2004) 67.
- [12] P. Deb, S. Ghosh, A. Basumallick, *J. Metall. Mater. Sci.* 43 (2001) 113.
- [13] A. Wiecher, R. Zach, Z. Kakol, Z. Tarnawski, A. Kozłowski, J.M. Honig, *J. Phys. B: Condens. Matter.* 359 (2005) 1342.
- [14] A. Miller, *Arz. Forsch.* 17 (1967) 921.
- [15] M.K. Wilson, *Infrared and Raman spectroscopy*, in: In F.C. Nachod, W.D. Phillips (Eds.), *Determination of Organic Structures by Physical Methods*, Academic Press, New York, 1962, p. 181.
- [16] J.R. Dyer, *Application of Absorption Spectroscopy of Organic Compounds*, Prentice-Hall of India, New Delhi, 1987, p. 22.
- [17] JCPDS file number 10-0325.
- [18] S. Enzo, G. Fagherazzi, A. Banedetti, S. Polizzi, *J. Appl. Cryst.* 21 (1988) 536.
- [19] Th.H.De.E. Keijser, E. Mittemeijer, H.C.F. Rozendo, *J. Appl. Cryst* 16 (1983) 309.
- [20] JCPDS file number 22-1189.
- [21] JCPDS file number 13-534.
- [22] P. Deb, A. Basumallick, P. Chatterjee, S.P. Sengupta, *Scripta Mater.* 45 (2001) 341.
- [23] S. Prasad, N.S. Gajbhiye, *J. Alloys Compd.* 265 (1998) 87.